Research Article

Nonlinear Modelling, Design, and Test of Steel Blast-Resistant Doors

V. A. Salomoni,[1] G. Mazzucco,[1] G. Xotta,[1] R. Fincato,[1] C. E. Majorana,[1] and M. Schiavon[2]

[1] *Department of Civil, Environmental and Architectural Engineering, University of Padua, Via F. Marzolo 9, 35131 Padua, Italy*
[2] *Wellco S.p.A. Engineering and Construction, Viale Mazzini 65/5, 31049 Valdobbiadene, Italy*

Correspondence should be addressed to V. A. Salomoni; valentina.salomoni@dicea.unipd.it

The nonlinear dynamic response for steel blast-resistant doors is here described, referring to an innovative experience at both national and international level requiring an ad hoc design and specific numerical simulations. The elements capability to sustain thermal loads due to fire hazards is additionally accounted for. The study has been conducted to define and characterize the nonlinear behaviour of a large number of doors, with the objective of sustaining dynamic loads from explosive hazards of fixed magnitude, as well as variable design and clearing times. The local overcome of the material strength limit (with correspondent plastic response) and possible formation of plastic hinges has been critically discussed. Numerical models have allowed for refining first design sketches and subsequently understanding the real thermomechanical behaviour for the investigated elements. Some experimental tests have been additionally performed, verifying the correctness of the already available numerical results, validating the adopted procedures, and correspondingly guaranteeing the doors' structural efficiency even under dynamic loads higher than design ones.

1. Introduction

The work takes its origin from a joint collaboration in the field of blast resistant buildings, doors, and windows. Particularly, steel doors and windows have been investigated considering that no predesigned elements could have been adopted; specification of gas plant locations and triggering material have been covered for privacy reasons. The response of steel/steel-glass structures due to a given blast wave is here described without focusing on its way of triggering or propagating [1].

Doors and windows effectively represent the most peculiar elements when designing blast resistant buildings; if building walls are capable to resist blast loads, the shock front may penetrate through doors and windows exposing people to sudden overpressure and fragments; additionally, building components not capable of resisting the blast wave will fracture and will be further fragmented and dragged by the dynamic flow following the shock front, causing other damage and problems [2, 3].

Another important aspect when dealing with blast doors and windows design is if reopening after explosion is requested for safety issues (i.e., escape of personnel after the blast) [4]. Such a requirement is largely binding, essentially in the numerical modelling phase, and its fulfilment is to be guaranteed by controlling specific parameters. It is hence possible to admit that doors and windows enter the plastic regime (also considering that Ultimate Limit States are accounted for [4]), but this asks for additional verifications of well-defined, norms-controlled ductility and rotation ratios. Consequently, the correct element behaviour is verified, and safety/rescue operations are ensured.

The designed, analysed, and produced doors (for brevity reasons, blast windows are not treated here) are of various types and dimensions, ranging from, for example, $1000 \times 2000 \, \text{mm}^2$ one-shutter door up to larger $3500 \times 4500 \, \text{mm}^2$ ones. Depending on doors and windows' dimensions as well as on their specific location, different peak blast loads and durations have been accounted for; nonlinear (for material and geometry) analyses have been conducted also

Table 1: Typical scheme of locations and loads for blast doors and windows.

	Location 1	Location 2	Location 3	Location 4	Location 5	Location 6	Location 7
Blast overpressure [psi]	0.406	0.710	1.500	2.176	2.610	3.000	4.340
Blast overpressure [bar]	0.028	0.049	0.103	0.150	0.180	0.207	0.299
Blast duration [ms]	70	59	33	65	45	45	80
DOOR type							
BD-01				X			
BD-1				X			
BD-2				X			
BD-3				X			
BD-4				X			
D1	X						
D3	X						
D4	X						
D6	X						
D1-S						X	
D4-S						X	
D5-S		X					
D8-S			X				
D11-S						X	
D21-S						X	
BSD-01					X		
BSD-02/03/06					X		
BSD-04/05					X		
BSD-02				X			
WINDOW type							
W1			X				
W2		X					
BSW-01/12					X		
P-3289	X						

considering frames, joints, plates, hinges, glasses, and opening devices. Procedures and methodology of analysis had already been known from a previous joint experience [5–7].

In the following, the main results related to one door type only have been reported, as well as the design, modelling, and testing lines followed in agreement with international recommendations [8–14]; additional details have been added referring to the inclusion of high temperature effects, for example, when the door is required to satisfy the Italian requirements for some fixed REI ("REI fire-rated door"): it ensures fire resistance, that is, the capacity to resist fire over a determined time period (expressed in minutes), and features stability ("R"), that is, the capacity to preserve the mechanical resistance; resistance to ("E") fire, steam, and hot gas emissions; thermal insulation ("I").

2. F.E. Modelling

2.1. Geometry. For the purposes described in the previous Section, suitable design criteria and procedures have been first fixed, as a starting point, in agreement with [15, 16]. Figure 1 depicts some typical doors and windows, originally defined by their dimensions only [5–7].

The designed locations of door and windows and corresponding pressure loads are reported in Table 1; due to the huge number of doors and windows to be built and the impossibility to define with certainty the final location per each structure, it has been decided to group them considering their geometric similarity and to refer to the maximum blast load.

As previously stated, the exact locations have not been indicated due to privacy reasons, and the triggering material has remained unknown to the authors; it has been anyway possible to refer to plane blast waves only, assumption which is clearly acceptable and true if the structures are sufficiently far from the triggering point [17–19]; correspondingly, a uniform distributed overpressure has been considered, as well as an orthogonal wave propagation with respect to the door/window plane (i.e., no reflected overpressure amplification has been included).

The reported assumptions and methodology are clearly not restricted to the specificity of the analyzed structure.

2.2. Models Construction. Finite element models have been set up to simulate the door behaviour in its closed configuration; beam-type elements have been used for defining

Figure 1: Typical design drawings of some representative door types.
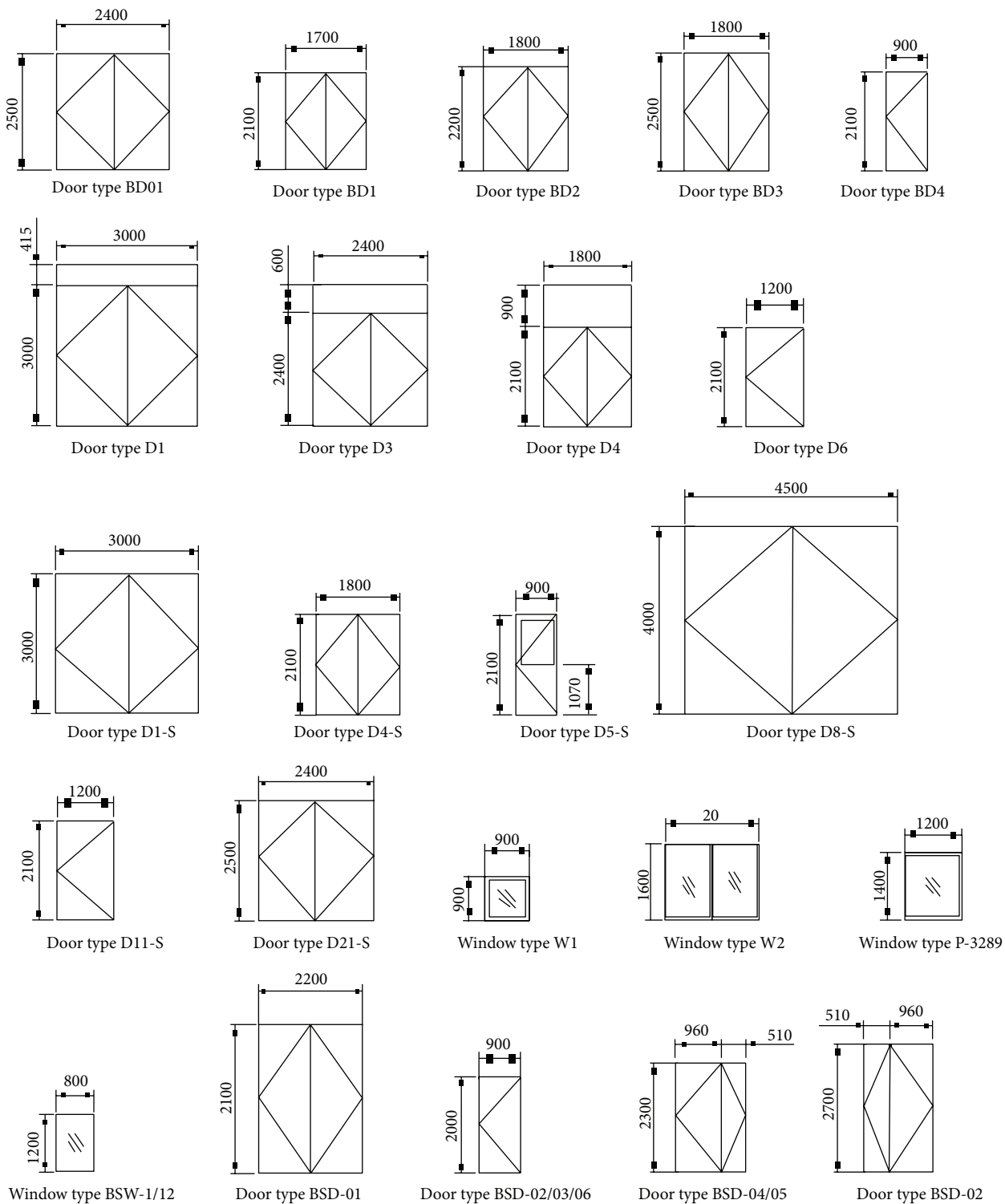
Note: all dimensions are reported in MM
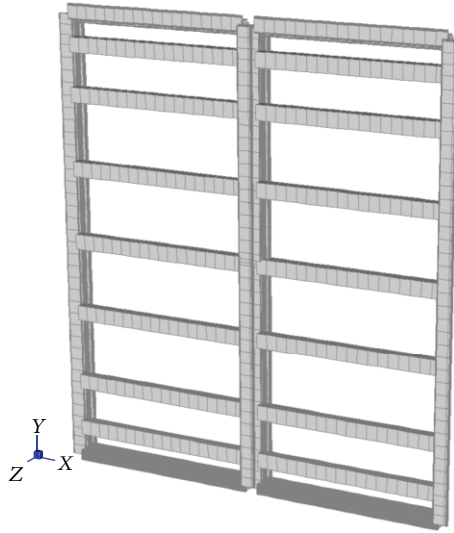
Figure 2: Main frame model, double shutter-type door.

Table 2: Steel mechanical properties.

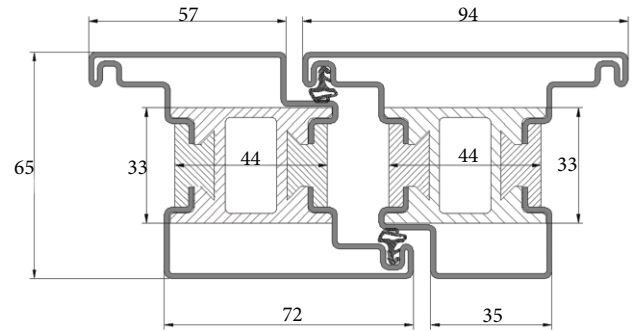|	
Elastic modulus [E]	210000 MPa
Yield stress [f_y]	235 MPa
Ultimate stress [f_u]	360 MPa

Figure 3: Typical internal and border elements.

Figure 4: Typical horizontal section.

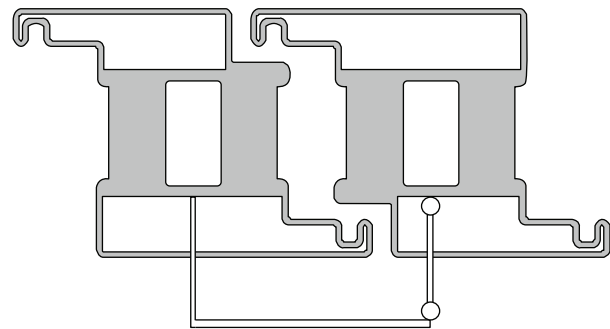
Figure 5: 3D model for counter-frame stiffness definition.

Figure 6: Shutter-to-shutter contact elements.

the main structure (frame), Figure 2, whereas shell-type ones have characterized the internal and external steel plates. The assumed mechanical properties of steel are showed in Table 2.

Beam elements present a transversal section in agreement with the design ones, to allow for defining a correct stiffness to internal and border elements (Figure 3); the number of horizontal stiffeners has been defined proceeding via a series of repeated analyses to obtain a structural response to guarantee the appropriate functional door behavior. Again, steel plates have been modeled to reproduce the design drawings (Figure 4).

2.2.1. Constraint Conditions. Each shutter is connected to the edge wall (through the counterframe) through hinges (which number has been determined again via repeated analyses), modeled with rigid constraints to allow for free rotations. The counterframe has been represented by the introduction of springs with equivalent stiffness, active in compression only; such a stiffness has been evaluated by considering a three-dimensional local model to which an imposed unit displacement has been applied (Figure 5). The contact between shutters has been additionally considered by interposing *link* elements, inactive if the response leads them to move away from each other (Figure 6), and closure points (representative of the real closure system, Figure 7).

During the *rebound* phase (qualifying the dynamic response and linked to the door bending in opposite direction with respect to the applied load), it has been assumed that the only active constraints are exclusively represented by closure points and hinges.

2.2.2. Dynamic Analyses. Once the (design) peak value of the blast load has been defined, as well as the time required for dissipating overpressure (t_d), specific values for peak reflected pressure (P_r), stagnation pressure (P_s), and clearing time (t_c) have been assumed, in agreement with recommendations, realizing diagrams of the type of Figure 8.

TABLE 3: Local verifications at ULS. (Step 315, $t = 0.03141$ s).

No beam	Section	Max N_s/N_{Rd}	$M_{s,11}/M_{Rd,11}$	$M_{s,22}/M_{Rd,22}$	V_s/V_{Rd}	$M_s/M_{N,Rd}$
110	2U_$60 \times 80 \times 60 \times 3$	0.0089	0.0015	0.0015	0.0081	0.0000
31	P1012	0.0124	0.0157	0.0024	0.0100	0.0003
20	P1013	0.0118	0.0106	0.0141	0.0045	0.0003
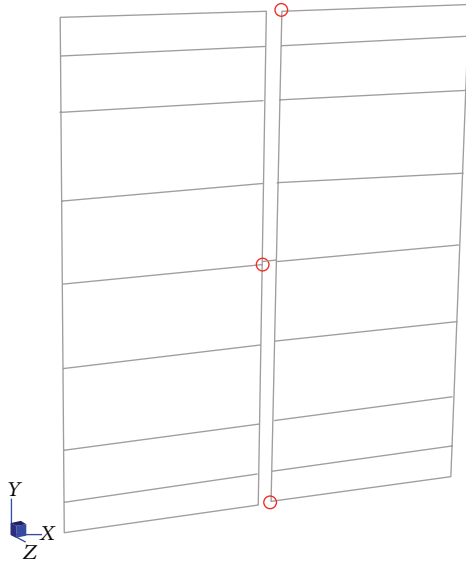
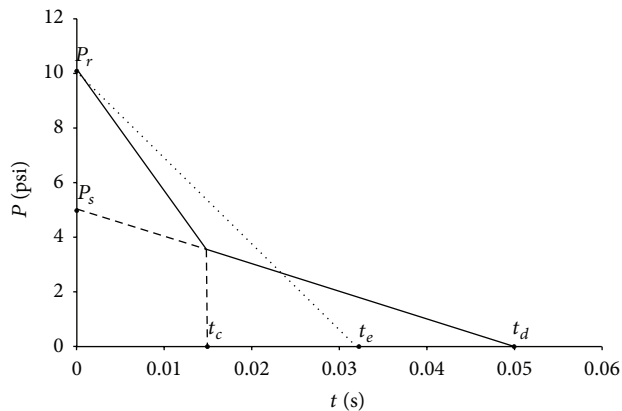FIGURE 7: Schematic representation of closure points (circles).

FIGURE 8: Typical pressure-time diagram for a plane frontal blast wave.

The analyses have additionally included effects of dynamic damping to take into account a possible reduction in stress deriving from internal frictions and yield of elements; particularly, damping effects coming from the formation of plastic hinges have been represented by assigning an elastoplastic behaviour to the material, whereas a fixed damping ratio has allowed for evaluating damping from internal frictions.

In Figure 9, a typical displacement evolution in damped and undamped configurations is reported (linear elastic response): the maximization of effects (peaks of maximum and minimum) is reached in both situations; this comes from the fact that the blast is rapidly exhausted (red curve) and the damping contribution is highlighted for longer times only (larger than t_d). Consequently, concerning the design phase, maximum actions only need to be considered and not the entire loading history; such an aspect has allowed for developing essentially undamped analyses, reducing computational times without loosing in approach generality and/or underestimating the real response.

2.2.3. Analysis of Results. For the typical door, the analyses have globally highlighted an elastic response both in the peak (Figure 10) and rebound phase (Figure 12) for the internal frame, with occurrence of out-of-plane displacements compatible with the correct structural behaviour of the whole door (essentially related to the door's reopening, see below). However, such a result is the consequence of initial pre-design assumptions and iterative simplified analyses to establish an initial configuration for which the response is just to be deepened and confirmed. Some local yield is anyway possible and acceptable as well in the frame itself, whereas even relevant yield of the steel plates (Figures 11 and 13) can be neglected considering that their key role is to transfer the load to the main frame, with no other structural function devoted to them.

Further, constraints reactions (varying with the structure oscillation consequent to the dynamic nature of the phenomenon) have been analysed and maximum values have been taken as reference; in general, internal hinges appeared to be overloaded, due to the door bending, and their verification has been developed in agreement with Eurocode 3 [20] (Figure 14); anchoring bolts of the perimetric counterframe have been checked as well.

It is to be noticed that, independently on the elastic or plastic door response due to blast, ultimate limit state calculations have been additionally performed [20], specifically conducting tension/compression, bending, and shear (and coupled actions) verifications for each section (see Table 3), automatically checked in case of a linear elastic global response; once a material nonlinear response had been evidenced (attainable, e.g., for larger doors and/or higher peak pressure values), such verifications could have failed so that, as stated, ductility and rotation ratios [11, 12] have been guaranteed to ensure reopening (unacceptable ratios leading to a door redesign and to repeated numerical analyses).

As a further design effort, a 3D hinge local model (Figures 15 and 16) has been implemented in order to check stress distribution and location of stress peaks; frame and counterframe have been modelled as well, separated by two rubber gaskets with mechanical properties as from Table 4.
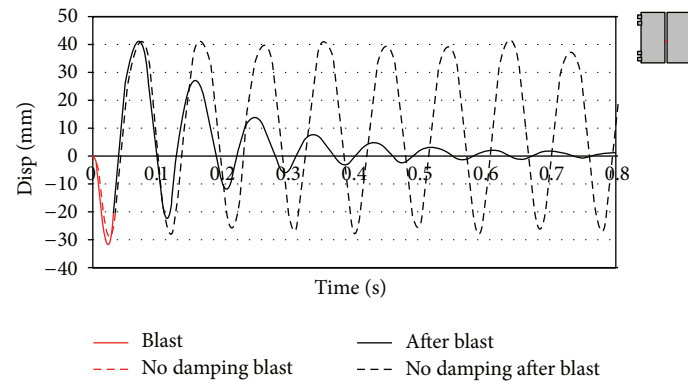
FIGURE 9: Typical displacement history for damped and undamped analyses.
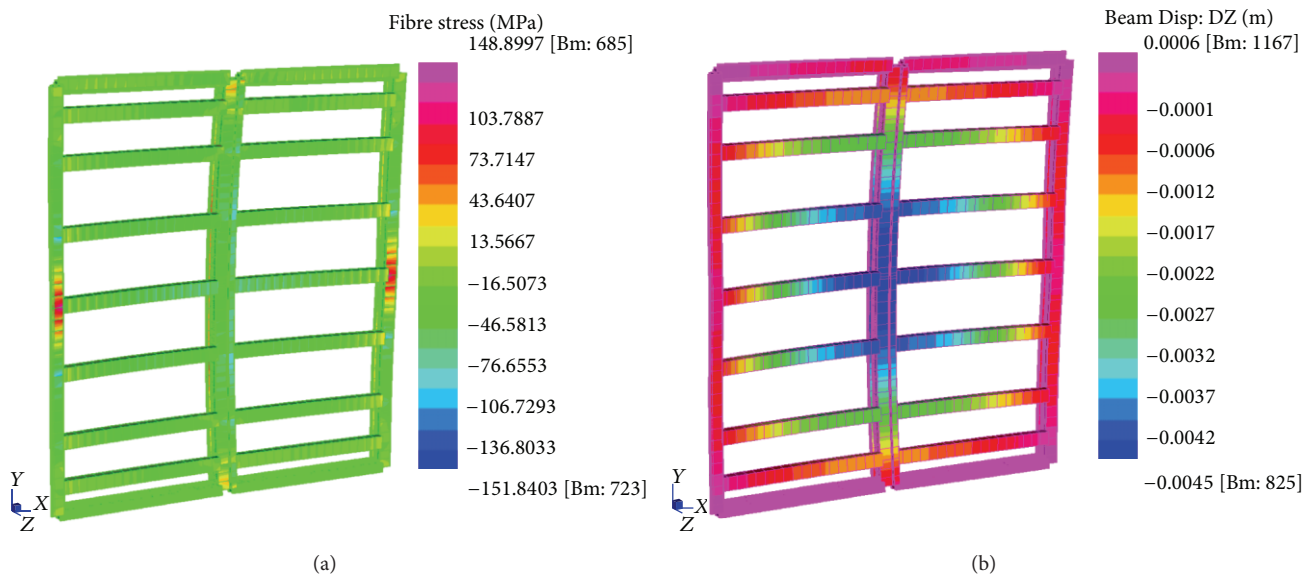

(a)

(b)

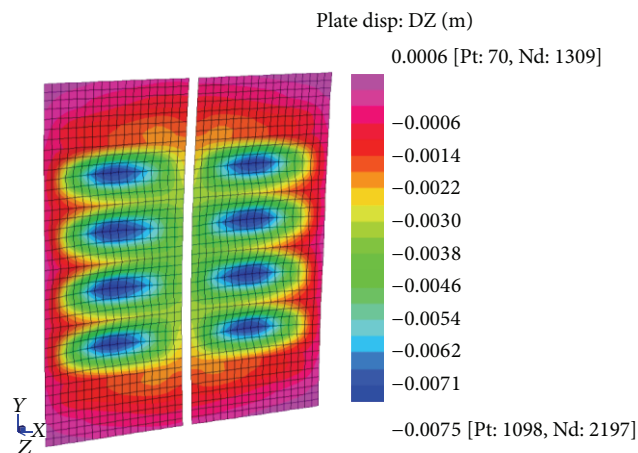FIGURE 10: Maximum stresses (a) and displacements (b) in the peak phase, internal frame.

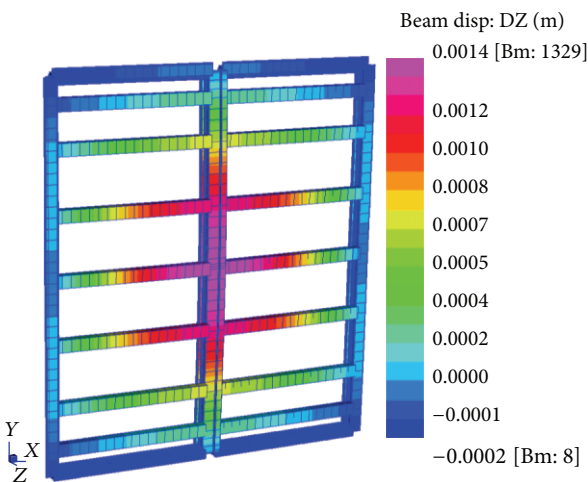FIGURE 11: Contour map of out-of-plane displacements during peak phase (steel plates).

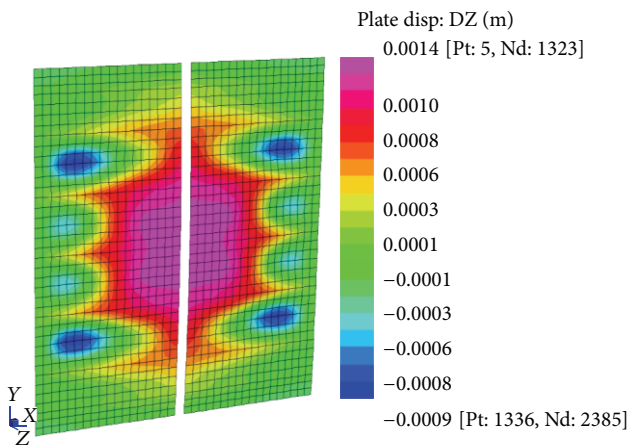FIGURE 12: Maximum displacements in the rebound phase, internal frame.

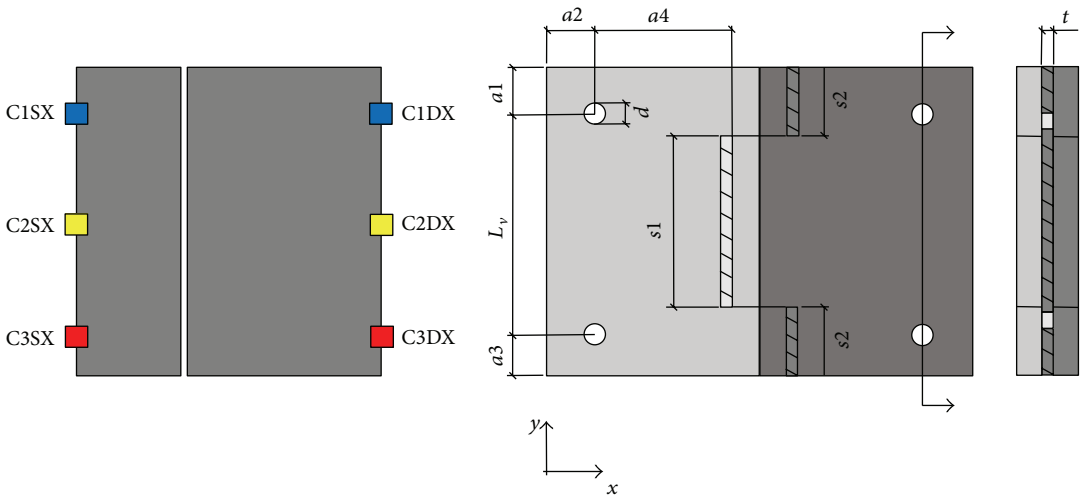FIGURE 13: Contour map of out-of-plane displacements during rebound phase (steel plates).

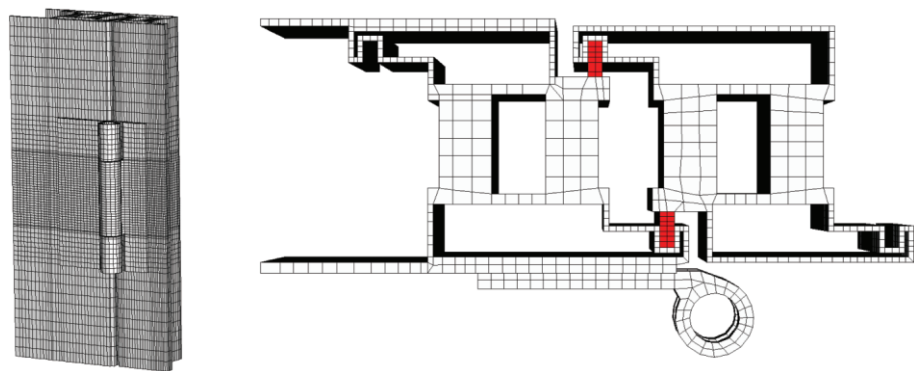FIGURE 14: Typical geometric scheme for hinges verification.

FIGURE 15: 3D local hinge model (portion), view and section.
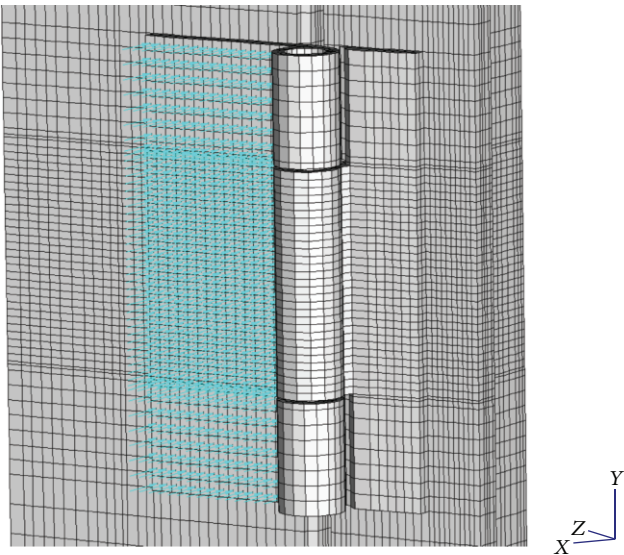
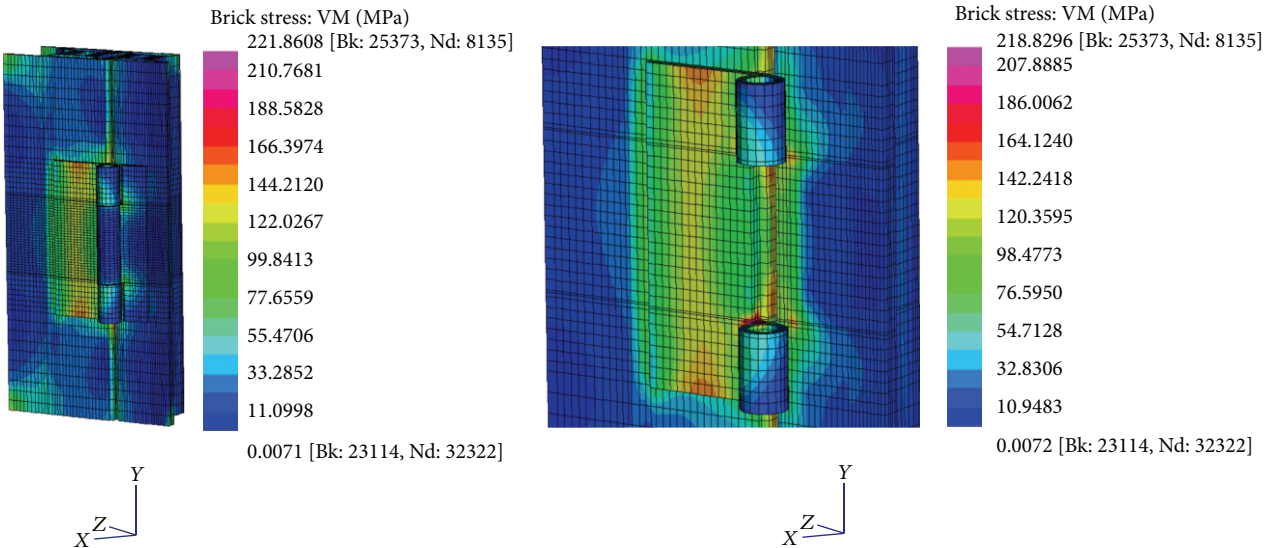

FIGURE 16: Pressure load on hinge.

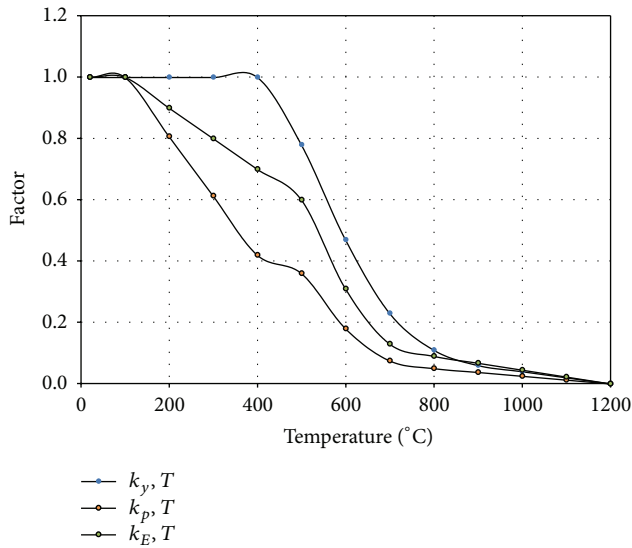FIGURE 17: Stress contour at peak step (detail on right).

FIGURE 18: Reduction factors (referring to yield stress, linear elastic limit, and Young's modulus) versus temperature.

TABLE 4: Rubber gaskets mechanical properties.

Elastic modulus [E]	80 MPa
Poisson's ratio [ν]	0.50
Density [ρ]	373.73 kg/m^3

Figure 17 shows stress values below the yield limit, confirming again that the steel response is in the elastic field for the whole analysis and for every component. The absence of plastic residual strains in the local model guarantees the complete functionality of the hinge after the blast wave impact, considering also that the plastic deformation of the frame satisfies the required ductility ratios.

2.3. The Inclusion of High Temperature Regimes. Under increasing temperatures, the steel mechanical characteristics deteriorate, as described by Eurocode 1 [21], so that reduction factors (ratios between mechanical characteristics at 20°C and at current temperature) are evaluated, leading to curves as in Figure 18 and, correspondingly, to stress-strain curves of the type of Figure 19.

The analysis (and subsequent verification) under fire has been conducted by developing two simplified models to describe the global structural behaviour. The first model assumes that the steel plate is directly exposed to fire, constrained by elastic springs (Figure 20). The stiffness of the springs has been evaluated considering the stiffness of the frame to which the plate is fixed; such a model allows for determining the stresses to be transferred to the door frame at different temperatures.

By applying a uniform thermal load to the plate, the plate tends to expand, but it is restrained by the frame stiffness. Such an inhibited deformation generates stress on the structure (Figure 21). Under an increasing thermal load, the increasing expansion produces higher stresses on
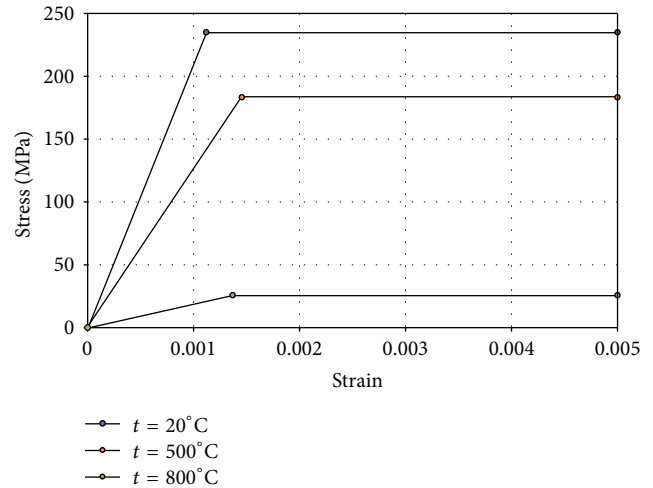

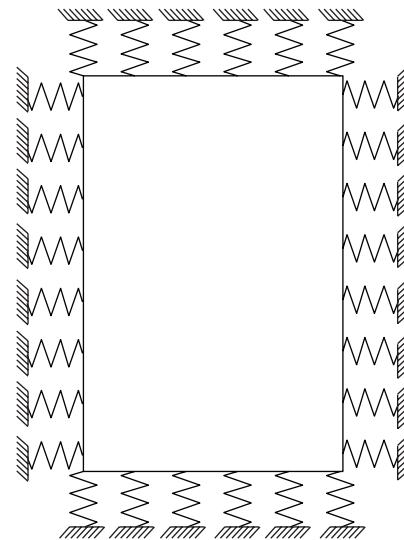FIGURE 19: Stress-strain diagram under variable temperatures.

FIGURE 20: Plate on elastic springs subjected to constant thermal expansion.

the frame up to reach the yield limit for the plate itself. Once the plate enters the plastic domain, being stresses constant (horizontal branch in Figure 19), it will transfer to the frame a constant load even if temperature continues to increase. Under a further increase in temperature, the mechanical characteristics decrease so that stresses in the frame are reduced (the strength limit being reduced itself). Consequently, for determining the maximum forces to which the frame is subjected during the door's transient heating, it must be defined when, at the lowest temperature—that is, with the highest mechanical characteristics—the plates transfer the maximum force to the frame. Hence, two verifications have to be generally conducted; the first to determine the maximum forces, at a temperature of 400°C (limit at which the plate maintains practically the same mechanical characteristics as at ambient temperature); the second instead considers the temperature configuration after 30 min when the plate exposed to fire is completely yielded.
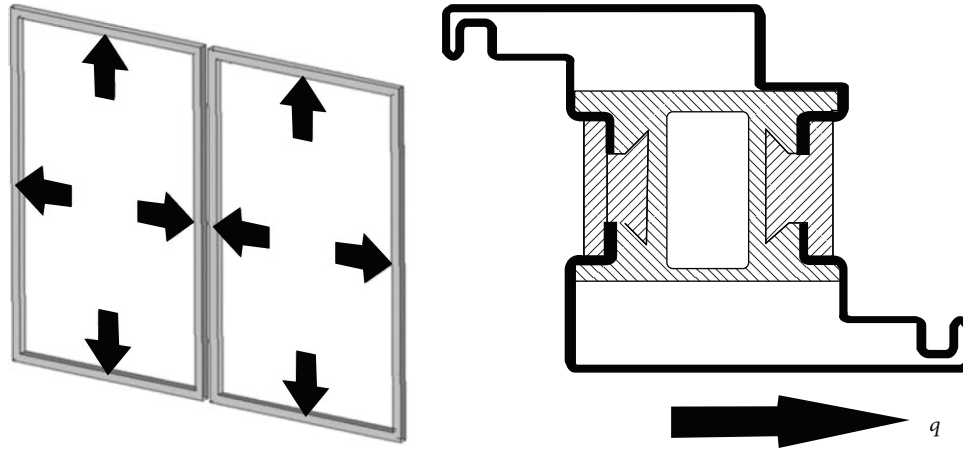
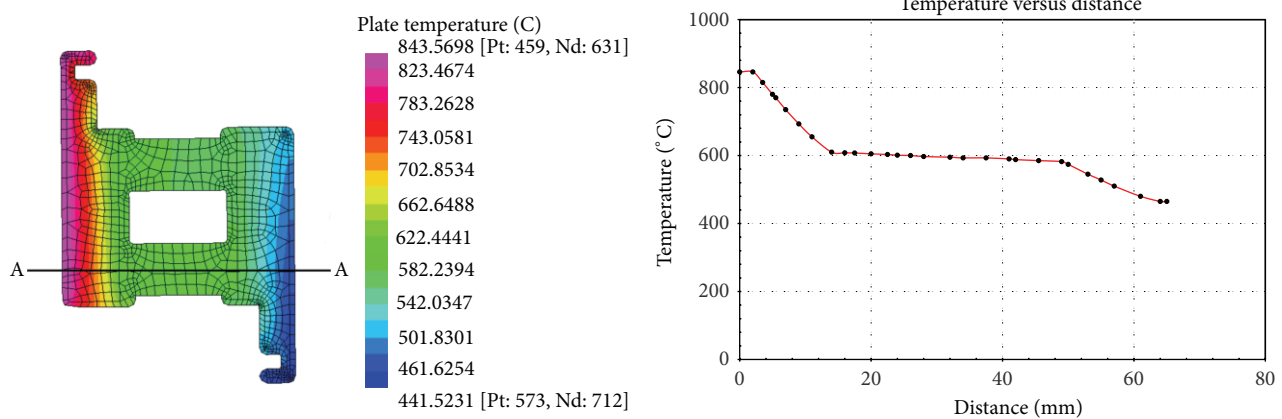FIGURE 21: Resulting action on the frame due to fire.

FIGURE 22: Temperature versus depth after 30 min.

The variation of temperature in the section after 30 minutes is shown in Figure 22.

3. Experimental Tests

An exact sample of a representative blast door (1:1 scale, $1800 \times 2100 \ mm^2$) has been built to check the door's effective strength and deformability under the design explosion conditions. The door has been tested so to ensure its structural performance and ability to sustain the stresses coming from a prescribed design blast load. It is expected that the door, even if possibly locally damaged, does not collapse and can be reopened after being subjected to such a blast. The environmental conditions have been reconstructed via an equivalent method exposed in the following (a similar approach can be found in [22]). The original plan and the basic hypotheses used for subsequently realizing the experiment are first recalled and derived from previous design work [5, 6, 23]; the discussion on the obtained results is then reported.

3.1. Description of the Test. The maximum value of the impact pressure has been planned to be reached through the test scheme of Figure 23; the explosion has been (dynamically) reproduced through the impact of a mass (with fixed weight) against the door. The nature of the impact is nearly local, not being the impact area diffused on the whole door, but such a condition can be assumed as more severe for evaluating the door's behaviour, so that the test has been in favour of safety (see also below). The design condition has been reproduced by means of energetic equivalences; that is, once fixed the weight of the impacting mass, the impacting height (or equivalently, the impacting distance measured in horizontal) comes out from imposing that the kinetic energy associated to the mass must equal the energy coming from the blast. Such energy is not referred to the released energy from the blast (which is unknown, the triggering point being also unknown and the explosive material), but equals the work done by the design pressure on the maximum displacement undergone by the door and numerically obtained (see before).

Via such an approach, the blast duration (or blast wave) has not been accounted for; even if such an assumption could lead to underestimate blast effects, it must be noticed that the underestimation could eventually affect the rebound phase only, but in any case, it can be considered negligible: in fact, the maximum displacement introduced in the energetic
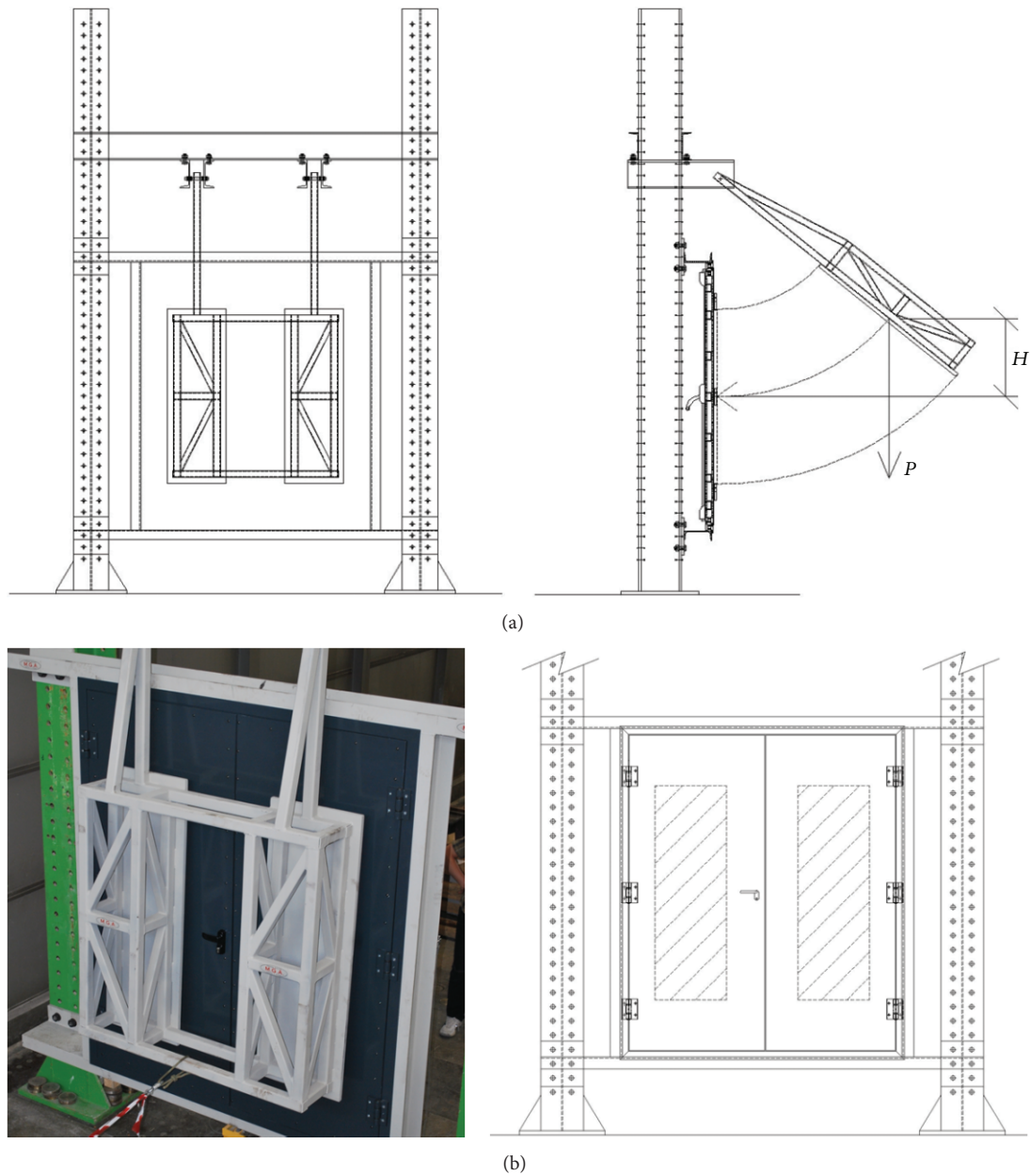
(a)

(b)

FIGURE 23: Sketch of the experimental test (top) and impact area.

equivalence is numerically obtained and consequently comes out from considering the real blast wave with the reflecting pressure (which is higher than the design blast pressure) and its duration as well. Again, it can be proved that a structure is more sensitive to a variation in the peak pressure rather than in a different time distribution of the blast wave. Hence, the blast wave has been assumed to reach the door with its peak value.

It has been also assumed that elastic responses and/or plastic dissipations (not quantifiable in the planning phase, due to the deformability of frames external to the door) are associated to a maximum of about 20% of the design energy. Such an aspect has been more deeply discussed in the following by analysing the results of the test.

The whole test has been conducted by means of successive steps, by incrementing the impacting height to reach higher heights to have a general idea on the "safety coefficient" associated to the constructed door.

Particularly, the calculated impacting (design) distance has been reached via one step only (essentially because the door is expected to be locally yielded under the design pressure, so that previous load steps could show permanent deformations which in reality would not be present); a subsequent step has been planned to verify that the door is able to sustain higher pressures.

Specifically, another numerical analysis (developed for such a purpose in an Ultimate Limit State) accounting for a higher blast pressure allowed us for determining a new

(a)

(b)

(c)

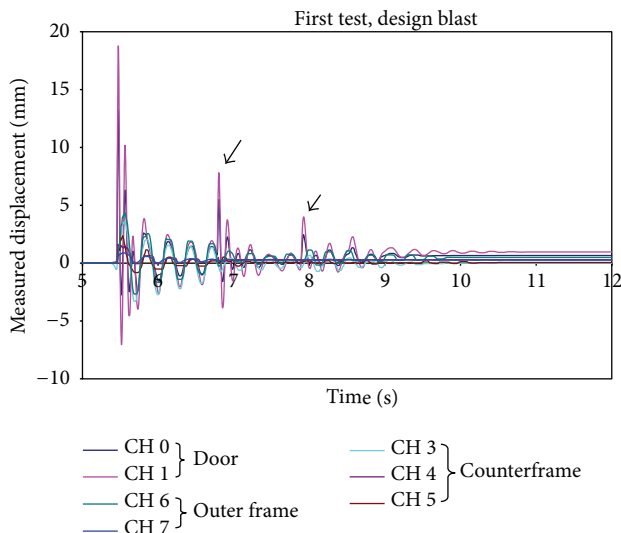FIGURE 24: ((a), (b), (c)) Location of transducers 4, 0–5, and 6-7.

FIGURE 25: Measured displacements.
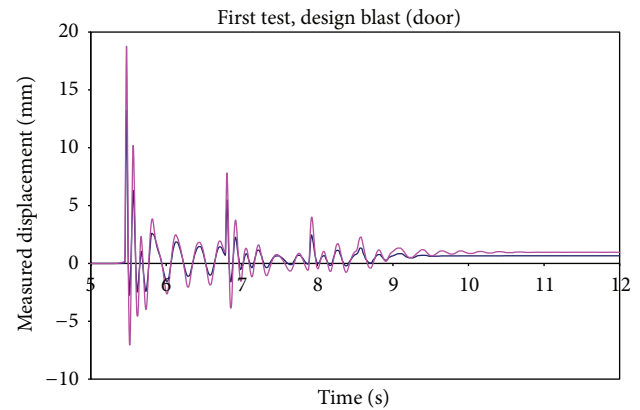
FIGURE 26: Measured displacements (door).

impacting distance (d_{MAX}), 1.7 times higher than the calculated design one. Hence, if the door is able to structurally respond to such an impact, it will be said to have an associated safety coefficient of 1.7 in ULS, with an associated energy about 3 times higher than the design one. Intermediate load steps, considering $d_{design} \leq d \leq d_{MAX}$, have been performed, having in mind that permanent deformations have already occurred under the design situation; in any case, such substeps would be associated to pressures in the fixed range.

In the configuration of d_{MAX} the door has not been instrumented, so avoiding possible damages to the adopted

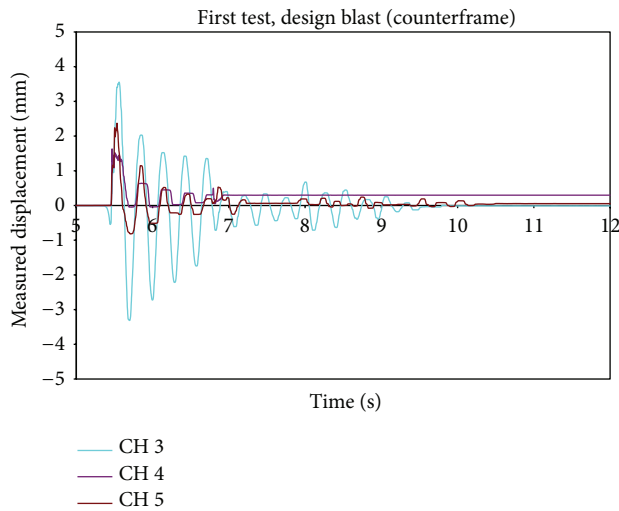First test, design blast (counterframe)

CH 3
CH 4
CH 5

Figure 27: Measured displacements (counterframe).

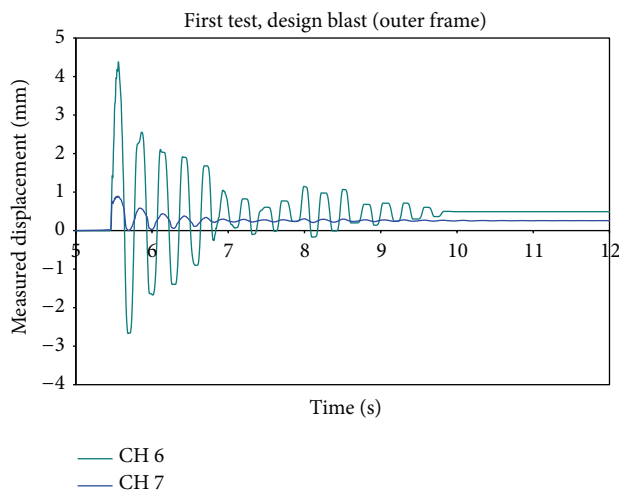First test, design blast (outer frame)

CH 6
CH 7

Figure 28: Measured displacements (main frame).

transducers (see below) due to the dynamic nature of the impact itself.

Displacement transducers (Table 5) have been located as in Figure 24; it has been decided to reach the design blast condition via one step only (in agreement with what previously stated); a second step has been performed by assuming an impact distance roughly corresponding to an intermediate blast pressure; a third test, not instrumented, has been performed as well just to check that the door is able to sustain about 1.5–2 times higher pressures without collapsing.

From the first test, some observations can be reported (Figure 25):

(i) the response of the whole system (door + counter-frame + main/green frame), and particularly of the door, is evidently damped, favourable condition for a structure which is devoted to respond to dynamic actions;

Table 5: Instrumentation technical features.

Multichannel measurement system brand HBM, model Spider8	
Main frequency	4,8 kHz per transducer
Precision	0.1
Maximum channels' number	8/device
Interface	Printer interface, RS-232
Data treatment	Low pass filter
Digital measurement step	9600 values/s
Inductive displacement transducers brand HBM, model W20	
Sensitivity [mV/V]	80
Nonlinearity and hysteresis	$\pm 0,2$ or $\pm 0,1$
Nominal displacement [mm]	20
Nominal range of temperature [˚C]	$-20 \cdots +80$
Main frequency [kHz]	$4,8 \pm 1\%$

(ii) the additional peaks in the displacements curve (black arrows) are the consequence of the repeated bouncing of the mass against the door; such an event acts anyway in favour of safety with the door additionally stressed by the bouncing itself;

(iii) the door's rebound is evidenced; it could be higher in reality due to effects of depressurization coming from the blast, but this aspect cannot be said to have consequences on the structural capability of the door to sustain the load. In any case, it does not affect at all the door's capability to be reopened after the blast.

By observing Figure 26, together with Figures 27 and 28, it appears that the "real" displacement undergone by the door is lower than the measured one, considering that counterframe and main frame represent deformable supports for the door itself.

Roughly speaking, counterframe and main frame act as springs in series, each one with its own stiffness; so, the effective door's displacement coming from the blast can be calculated by subtracting the displacements undergone by counterframe and main frame to the measured door's displacement.

Hence, considering just the maximum values and assuming that the measured displacement for counterframe and main frame are mean values, the maximum design door's deflection has been calculated; having in mind the overestimation due to a concentrated load, the effective door's deflection has been updated, and the associated energy has been found to be very close to the estimated one.

As reported by Figure 29, under the design blast, the door has been easily reopened.

For sake of brevity, just the final results of the second and third tests are reported and commented: the door reveals a moderate stiffer behaviour during bound and a less stiff behaviour during rebound; the door has assumed a deformed permanent configuration due to the previous blast which has modified its structural response giving rise to smaller displacements; the entrance in the plastic field is still small but

FIGURE 29: Door's reopening after blast.

more evident than in the previous situation; the counterframe and main frame's deformation starts to be no more negligible.

From calculating the energy associated to this load-step as well as the corresponding pressure and impact distance, it directly comes out that essentially a linear relationship exists between impact distance and applied force (which generally is not the case): this can be said to be a consequence of an essentially linear elastic behaviour for the door. By extension (even if such an assumption loses validity as loads increase), the blast pressure related to the last test has been directly evaluated from the impact distance by proportion.

As in the previous test, the door could be easily reopened.

In the last test door, counterframe and frame have revealed (visible) relevant displacements, and the deformations undergone by the door are surely underestimated by such a test (due to the deformability of counterframe and frame). But no specific structural significances have been attributed to the test, apart from realizing that the door is able to sustain pressures higher than 1.5–2 times the design one. The door could be reopened even after this impact.

4. Conclusions

Numerical analyses have been briefly described, referring to an innovative experience, at both national and international level, dealing with modelling, designing, and realizing steel blast-resistant doors.

The study has been conducted to define and characterize the nonlinear response of a large number of doors (and windows) with steel frame, with the objective of sustaining dynamic loads from explosive hazards of fixed magnitude and variable design and clearing times.

The local overcome in the strength limit (i.e., generating a plastic response) and possible formation of plastic hinges have been critically discussed and examined in relation to prescribed regulations and recommendations.

The numerical models have allowed for refining first design sketches and subsequently understanding the real structural behaviour of the investigated structures. Their capability to sustain thermal loads due to fire hazards has been additionally accounted for.

Experimental tests on typical steel doors at 1:1 scale have been conducted with the objective of "a posteriori" verifying the correctness of the already available numerical results, validating the adopted procedures, and correspondingly guaranteeing the doors' structural efficiency even under dynamic loads higher than design ones.

Acknowledgment

References

[1] D. K. Ofengeim and D. Drikakis, "Simulation of blast wave propagation over a cylinder," *Shock Waves*, vol. 7, no. 5, pp. 305–317, 1997.

[2] J. Leppänen, "Experiments and numerical analyses of blast and fragment impacts on concrete," *International Journal of Impact Engineering*, vol. 31, no. 7, pp. 843–860, 2005.

[3] D. J. Forbes, "Blast loading on petrochemical buildings," *Journal of Energy Engineering*, vol. 125, no. 3, pp. 94–102, 1999.

[4] ASCE Report, *Design of Blast Resistant Buildings in Petrochemical Facilities*, ASCE, New York, NY, USA, 1998.

[5] C. E. Majorana and V. A. Salomoni, "Preliminary design and numerical analyses of steel blast doors and windows," in *Proceedings of the 5th Asia Pacific Conference, Shock and Impact Loads on Structures*, pp. 301–307, 2003.

[6] V. A. Salomoni, "Predicted responses of structures subjected to blast and blast-induced phenomena," Proceedings of the 2nd International Conference on Protection of Structures Against Hazards, Singapore, 2004.

[7] C. Majorana, V. Salomoni, and T. S. Lok, Eds., *Proceedings of the 3rd International Conference on Protection of Structures against Hazards, Venice, Italy, 28-29 September 2006*, CI-Premier Pte Ltd., Singapore, 2006.

[8] UNI EN 13541:2000, *Glass in Building—Security Glazing—Testing and Classification of Resistance Against Explosion Pressure*, 2000.

[9] UNI EN 572-1:2004, *Glass in Building—Basic Soda Lime Silicate Glass Products—Part 1: Definitions and General Physical and Mechanical Properties*, 2004.

[10] prEN 13474-2 (CENT/TC129/WG8), *Glass in Building—Design of Glass Panes—Part 2: Design for Uniformly Distributed Loads*, 2000.

[11] PIP STC01018, *Blast Resistant Building Design Criteria*, 2006.

[12] AISC Steel Construction Manual, *Specifications for Structural Steel Buildings*, 13th edition, 2005.

[13] AISI S100-2007, *North American Specifications for the Design of Cold-Formed Steel Structural Members*, 2007.

[14] ACI 2007, *Building Code Requirements for Structural Concrete and Commentary (Includes Errata)*, ACI 318-07, American Concrete Institute Code, 2007.

[15] Naval Facilities Engineering Command, *Blast Resistant Structures—Design Manual 2.08*, Philadelphia, Pa, USA, 1986.

[16] BP International Limited, Research & Engineering Centre, *Procedure For the Design of Buildings Subject to Blast Loadings. RP 4-6*, BP Group Recommended Practices and Specifications for Engineering: Engineering Practices Group, Sunbury-on-Thames, UK, 1993.

[17] B. Luccioni, D. Ambrosini, and R. Danesi, "Blast load assessment using hydrocodes," *Engineering Structures*, vol. 28, no. 12, pp. 1736–1744, 2006.

[18] X. Q. Zhou and H. Hao, "Prediction of airblast loads on structures behind a protective barrier," *International Journal of Impact Engineering*, vol. 35, no. 5, pp. 363–375, 2008.

[19] I. G. Cullis, "Blast waves and how they interact with structures," *Journal of the Royal Army Medical Corps*, vol. 147, no. 1, pp. 16–26, 2001.

[20] UNI EN 1993-1-1, *Eurocode 3; Design of Steel Structures; Part 1-1: General Rules and Rules for Buildings*, 2005.

[21] UNI EN 1991-1-2, *Eurocode 1; Actions on Structures; Part 1-2: General Actions—Actions on Structures Exposed to Fire*, 2004.

[22] P. Huson, R. J. Asaro, L. Stewart, and G. A. Hegemier, "Non-explosive methods for simulating blast loading of structures with complex geometries," *International Journal of Impact Engineering*, vol. 38, no. 7, pp. 546–557, 2011.

[23] V. A. Salomoni, G. Mazzucco, G. Xotta, R. L. Fincato, M. Schiavon, and C. E. Majorana, "Non-linear modelling, design and production of steel blast-resistant doors and windows," in *Proceedings of the 4th International Conference on Computational Methods for Coupled Problems in Science and Engineering*, pp. 548–558, Kos Island, Greece, June 2011.